An active, high bandwidth, flexible connector for large area computational systems

Randall Irwin
UCLA Center for Heterogeneous Integration and Performance Scaling
Los Angeles, USA
randall.irwin@ucla.edu

Joanna Fang
UCLA Center for Heterogeneous Integration and Performance Scaling
Los Angeles, USA
joannafang@ucla.edu

Subramanian S. Iyer
UCLA Center for Heterogeneous Integration and Performance Scaling
Los Angeles, USA
s.s.iyer@ucla.edu

***Abstract*—Large area computational systems such as systems-on-wafer (SoWs) require high bandwidth communication links to the outside world. Commercial high bandwidth cabling solutions are incompatible with integration to SoWs due to large plastic connector interfaces. FlexCon, a flexible, high bandwidth connector cable platform, features high density interconnects on a highly flexible, elastomeric substrate integrable with SoWs via conventional reflow processes. However, losses in FlexCon channels limit the maximum reach of FlexCon. Here, we demonstrate two methods of improving the reach of FlexCon. First, the lossy SU-8 dielectric is replaced with a low-loss parylene-N dielectric, reducing losses by 32%. Second, an active linear redriver was implemented on FlexCon via a surface mount assembly process. Process development of direct integration of the linear redriver in the FlexCon substrate is discussed. Additionally, the reliability of FlexCon channels under cyclic mechanical bending is investigated. Changes in insertion loss after 1000 cycles at a bending radius of 2.5mm was found to be <6% at high frequency.**

Keywords— flexible connector, system-on-wafer, high bandwidth, bending.

I. INTRODUCTION

Recent advances in artificial intelligence (AI) and machine learning (ML) have been driving demand for compute and memory in high performance computing systems (HPCs) to extreme levels. Large language model (LLM) parameter count is trending beyond 1 trillion, necessitating advanced HPCs for accelerated training. Systems-on-wafer (SoWs), such as the Silicon Interconnect Fabric [1], leverage mature CMOS processing techniques and advanced packaging technologies, e.g., hybrid or thermocompression bonding (TCB), to achieve tight interconnect and bonding pitch for high performance, heterogeneously integrated systems with high inter-die bandwidth and low latency.

SoW-based HPCs are poised to meet the growing needs of AI/ML applications, however, practical implementation requires connections to the outside world. Data transfer between the SoW and a PCB or a second SoW in a multi-wafer system can be realized through direct connection using metal or optical links, or wirelessly with RF links. For optical links, valuable silicon area must be used for v-grooves or diffraction gratings, waveguides, modulators and demodulators, photodetectors, and transimpedance amplifiers (TIAs). Wireless RF links have similar challenges, reducing the effective area for compute and memory on the SoW. In contrast, metal interconnects in the form of a cable require minimal area for the connector interface. However, commercial high bandwidth cables typically use bulky plastic connectors which are incompatible with direct silicon integration due to high mismatch in coefficients of thermal expansion (CTEs) between the silicon and the connector. Furthermore, aggregate bandwidth requirements for a 300 mm SoW can exceed 200 Tbps, for which commercial solutions are lacking.

To address these challenges, we have been developing FlexCon, a high bandwidth flexible connector cable platform with 240 Gbps/mm shoreline bandwidth, capable of providing >200 Tbps aggregate I/O on a 300 mm SoW [2,3]. FlexCon leverages the die-first fan-out wafer-level packaging (FOWLP) process for FlexTrate^{TM}, a flexible hybrid electronics platform, to achieve fine-pitch wiring on an elastomeric PDMS substrate with integrated active components [4]. The capability of directly integrating components into FlexCon provides the key advantage of moving components from the SoW, e.g., SerDes, which would otherwise occupy silicon area.

Previously, we have demonstrated passive channels on FlexCon using a SU-8 dielectric with < 6 dB insertion loss over 20 mm [3]. For applications requiring longer reach at a comparable insertion loss, modifications to FlexCon are necessary. Passive channel losses are due to conductor and dielectric losses. Conductor losses can be reduced by increasing the conductor size, thereby reducing resistance, but this is a tradeoff with signal conductor density. For a given conductor geometry, conductor losses can be reduced only by reducing surface roughness via process optimization. On the other hand, dielectric losses can be reduced by selecting and implementing a low-loss material.

For scenarios in which passive channel loss remains too high, active components such as signal buffers and repeaters can be implemented to compensate for lossy channels. Linear redrivers provide signal buffering and programmable equalization to boost high frequency signals, offsetting frequency-dependent losses.

In this work we, demonstrate two methods of increasing the reach of the FlexCon channel: replacing the lossy SU-8 dielectric with low-loss parylene-N and implementing an active

This work was supported in part by NSF WaSCoS award #223109 and NSF Eager award #222646.

2377-5726/24/$31.00 ©2024 IEEE
DOI 10.1109/ECTC51529.2024.00299

linear redriver to buffer signals. Additionally, the reliability of FlexCon is investigated via a cyclic mechanical bending study. In Section II, we provide the experimental details for each of the studies conducted, including fabrication processes. In Section III, we provide and discuss results of each study. The paper is concluded in Section IV.

II. Experimental

FlexCon was developed on the FlexTrate™ platform, which applies FOWLP techniques to enable flexible, heterogeneously integrated electronic systems. The process flow for the three FlexCon configurations demonstrated here, is shown in Fig. 1.

A. *FlexCon with low-loss Parylene-N dielectric*

TABLE I. Candidate Dielectric Properties

Property	SU-8 [5]	Polyimide	Parylene-N [6]
Dielectric Constant	3.2	3.3	2.65
Loss Tangent	4E-2	2E-3	6E-4
Young's Modulus	2.0 GPa	2.4 GPa	2.4 GPa
Tensile Strength	60 MPa	128 MPa	48.3 MPa
Elongation	6.5%	10%	2.5%
Cure/Dep. Temperature	95°C	>200°C	RT

As stated previously, losses in FlexCon channels can be reduced by implementing a low-loss dielectric as a replacement for the lossy SU-8 dielectric. A suitable alternative material requires the following properties: low dielectric constant to minimize RC delay; low loss tangent; mechanical flexibility; low processing temperature (<200 °C); and processability. Some potential material candidates are shown in Table I. Polyimide is commonly used in a variety of microelectronics applications but requires a high cure temperature incompatible with the FlexCon process. Alternatively, Parylene-N has a loss tangent two orders of magnitude lower than SU-8, can be deposited at room temperature, and has mechanical properties comparable to SU-8. For these reasons parylene-N was selected as a replacement for SU-8.

The fabrication process for FlexCon with parylene-N is shown in Fig. 1a. Following deposition of the ground plane layer, 13 μm of parylene-N is deposited and patterned using a 100 nm Al hard mask and O_2 RIE. Vias are plated up followed by semi-additive wiring metallization. The assembly is passivated with 2 μm of parylene-C, and contacts are opened via RIE and passivated with 20/200 nm of Ti/Au.

B. *Active FlexCon*

1) *Surface mount assembly*

To ensure high flexibility and reliability, components implemented on the FlexTrate™ platform are in bare die form. Compared to packaged dies, bare dies occupy significantly lower area and are much thinner. Area and thickness reduction provide several benefits: lower stress near components under bending; lower die shift during molding; reduced warpage; improved flexibility; and lower thermal resistance [7]. Sourcing off-the-shelf components in bare die form remains a persistent challenge in developing new applications on the FlexTrate™ platform, but improvement is expected as the chiplet ecosystem gains traction.

In high speed signaling applications, improving channel reach can be achieved using active signal buffers or repeaters with equalization. These components recover and drive signals in lossy channels at the cost of increased energy consumption and latency. In this demonstration we employ a linear redriver (Texas Instruments SN75LVPE4410), which features four channel buffering and continuous time linear equalization (CTLE) for PCIe 4.0 applications. However, this component is available only in packaged form. To demonstrate functionality on FlexCon, we first opted to implement the redriver as a surface mount assembly. Other components used in this assembly were

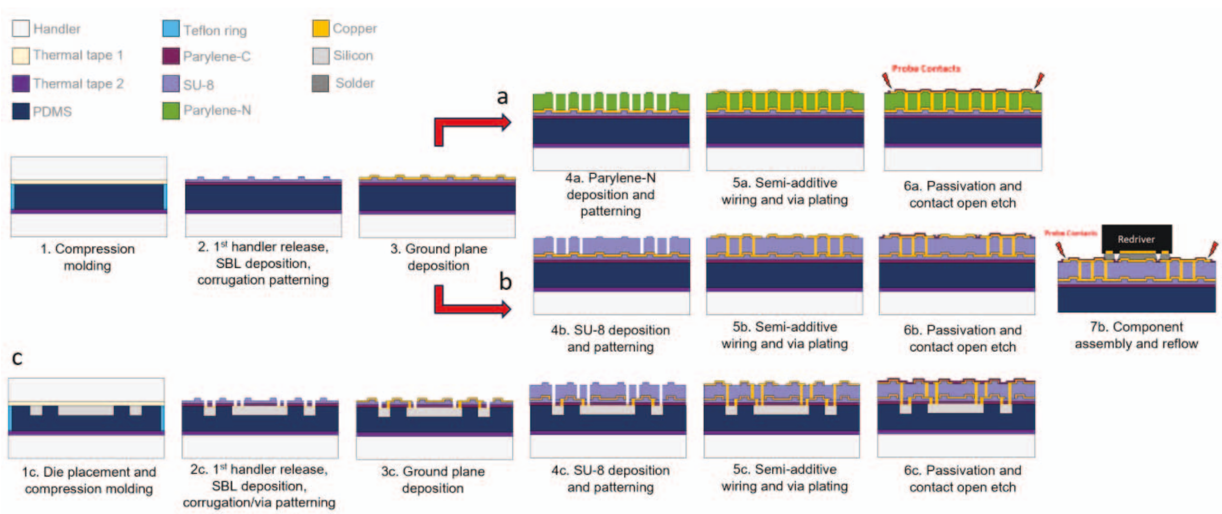

Fig. 1. FlexCon process flows. a) Passive FlexCon with parylene-N. b) Active FlexCon with surface mount assembly. c) Active FlexCon with integrated depackaged bare die.

one 4.7 kΩ resistor, one 59 kΩ resistor, and two 100nF capacitors.

The fabrication process flow for this assembly is shown in Fig. 1b. Following fabrication of FlexCon, components were mounted and assembled using a low temperature SnBiAg solder paste reflow process. A top view of the final assembly is provided in Fig. 2. The redriver was placed in the center of a 44.5mm channel. Pads at the top of the image were used to deliver power and program the redriver.

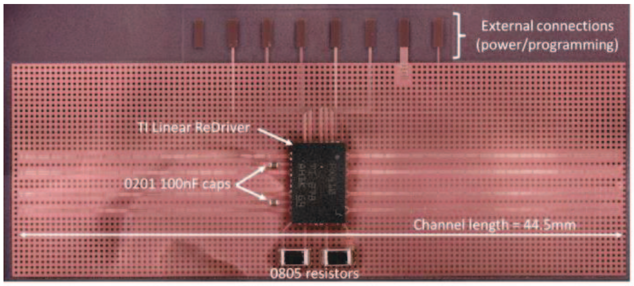

Fig. 2. Top view of active FlexCon surface mount assembly.

2) Chip depackaging and bare die integration

As stated above, integrating the linear redriver by embedding the packaged chip in the PDMS substrate leads to several fabrication and reliability challenges. As such, first removing the die from the package is necessary prior to integration. Several depackaging techniques are available, such as chemical wet etching with various acids [8], dry etching via RIE, mechanical etching, or a combination of these. The slow etch rate of RIE proves costly and time consuming due to potentially hundreds of microns of epoxy needing removal. Mechanical etching can remove epoxy quicker, but also easily damage the die. For these reasons, we opted for wet etching to depackage the redriver.

Compatible acids must be selected to avoid damage to the die, e.g., etching pads and interconnects. Cross sectioning the chip revealed that the die pads were composed of aluminum and connected to the chip pads via copper wirebonds. Nitric acid and sulfuric acid have been shown to effectively remove epoxy but can react with copper and aluminum. Nitric acid readily attacks copper, especially at elevated temperatures, while sulfuric acid does the same to aluminum. Concentrated nitric acid is known to form a passivation layer on aluminum, preventing etching.

As the wirebonds were intended to be removed prior to integration, red fuming nitric acid heated to 80 °C was first tested for depackaging. However, it was found that the copper interconnects on the die were being etched before all the epoxy could be removed. Concentrated sulfuric acid (96%) at 155 °C was next tested and was found to effectively remove epoxy with minimal effect to the copper wirebonds and interconnects but etched the die pads prior to complete removal of epoxy. A shorter duration in sulfuric acid was found to etch the epoxy to below the surface of the die, but not completely remove all epoxy, while ensuring the pads remained intact. Unremoved epoxy on the leadframe was measured to lie below the die surface by ≥100 μm, expected to be suitable for integration. Intact wirebonds were removed using dilute APS-100 copper

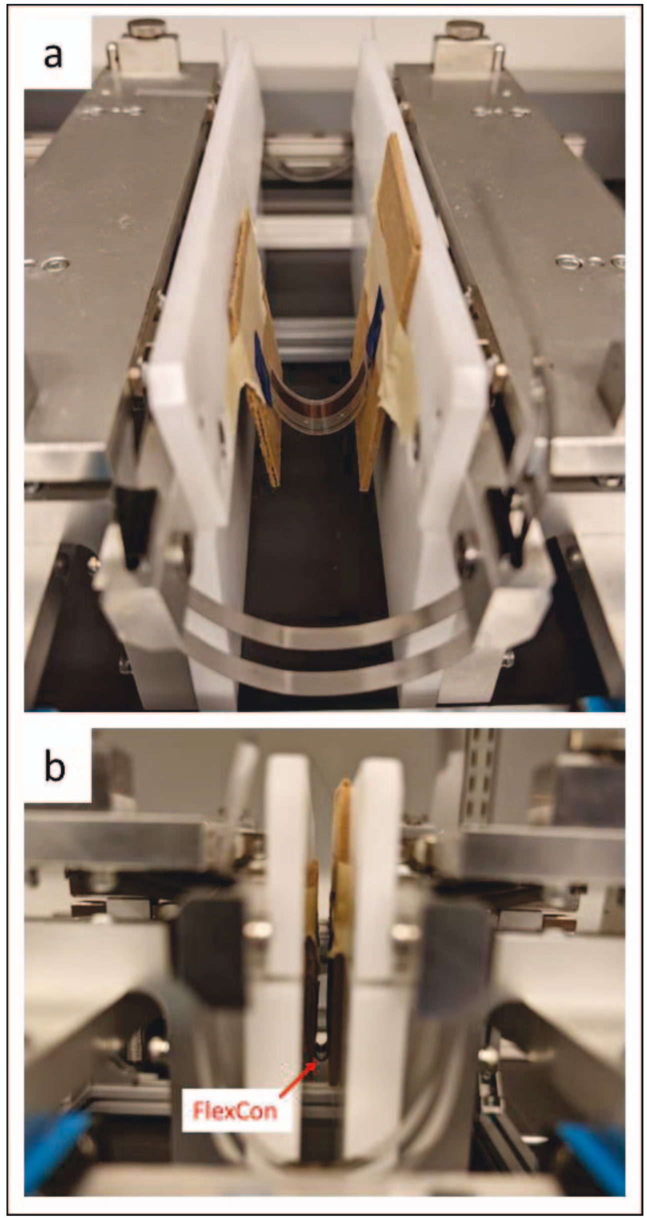

Fig. 3. a) FlexCon mounted in the bending tool and b) bent to 5 mm bending radius.

etchant and ultrasonication. To compare the effect of complete removal of epoxy and aluminum pads to the effect of incomplete epoxy removal with intact pads, both configurations were integrated in FlexCon.

The process flow for the bare die integration of active FlexCon is shown in Fig. 1c. The depackaged redriver and passives were first aligned and placed onto a handling wafer laminated with a thermally releasable adhesive. After compression molding, the first handler was thermally released. Redriver pads were plated via a semi-additive process to ensure contacts for the samples in which the aluminum die pads were etched off. Subsequent steps follow the standard process flow.

Resistance of each redriver pad with respect to ground were measured at each step to ensure connectivity and screen for potential issues.

C. Cyclic mechanical bending study

The bendability of FlexCon is key to ensuring reliable signaling in practical applications. FlexCon may be used, for example, to connect adjacent, non-coplanar or stacked systems. In such scenarios, FlexCon may be bent during operation, and repeatedly bent during handling and assembly.

Evaluation of the effect on DC resistance of repeated bending of FlexTrate™ interconnects at various radii has been previously performed using a U-shaped folding tester [4]. In contrast to the standard FlexTrate™ platform, FlexCon features an additional metal layer and higher total dielectric thickness and is intended for use in high frequency applications. As such, the bending study was repeated on passive FlexCon channels of 44.5 mm length with SU-8 dielectric to determine the effect on insertion loss. Fig. 3 shows the sample mounted in the tester. Bending radii tested were 10 mm, 7.5 mm, 5 mm, 2.5 mm, and 1 mm at 1,000 cumulative cycles per radius.

D. Electrical characterization

The S-parameters of FlexCon in each of the above studies were measured using an Agilent N5247A PNA-X vector network analyzer (VNA). Cascade Microtech 50µm GSSG Infinity probes were used to contact the channels. Calibration of the VNA was performed prior to measurement using the short-open-load-thru method with an impedance standard substrate.

III. Results and Discussion

A. FlexCon with low-loss parylene-N dielectric

The insertion loss of passive FlexCon channels with Parylene-N is shown in Fig. 4. The measured loss is higher than expected based on simulations, suspected to be caused by surface roughness. For a given wiring geometry, i.e., conductor thickness, width, and spacing, the characteristic impedance is determined by the dielectric constant and thickness of the dielectric layer. For parylene-N, this thickness is ~11.5 µm. In contrast to SU-8, which can be deposited at the desired thickness with appropriate spincoating parameters, parylene-N is deposited via chemical vapor deposition (CVD) which has some variation. To accommodate for process tolerances, the nominal deposition thickness was selected as 13 µm. RIE was performed to reduce the layer thickness, resulting in roughness to the dielectric surface. Consequently, the underside of the wiring is rougher than desired, resulting in higher losses. Reduction of this roughness can be achieved via optimization of the RIE parameters, or spincoating a thin planarization layer.

In addition to the losses due to roughness, we observe dips in the insertion loss. Inspection of the channels revealed processing defects involving the ground vias, in which the plated wiring surrounding a small number of vias was missing, as shown in Fig. 5. It is suspected, but not confirmed, that this is due to a combination of poor adhesion of the metal to the parylene-N and localized stresses near vias resulting in delamination. These discontinuities along the signal path are believed to result in the effects observed here.

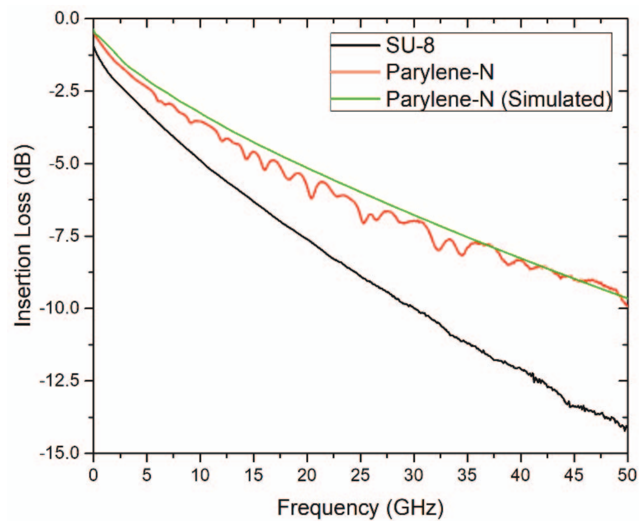

Fig. 4. Insertion loss of passive FlexCon channels comparing SU-8 and Parylene-N. Channel length = 44.5 mm.

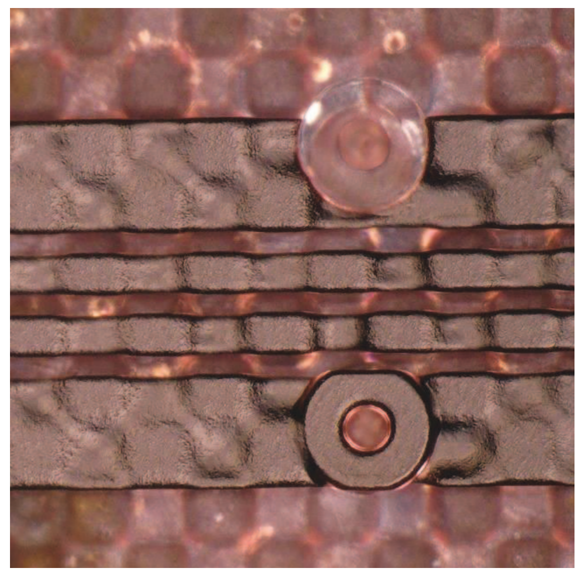

Fig. 5. Process defect during fabrication of FlexCon with parylene-N dielectric in which a ground via is unplated.

Despite the fabrication issues, we observe a reduction in insertion loss of ~32% at 32 GHz compared to SU-8, enabling an increase in reach of 12mm. Process optimization to reduce surface roughness and eliminate defects is expected to further reduce losses to ~54% of SU-8 losses, enabling an increase in reach of 21 mm.

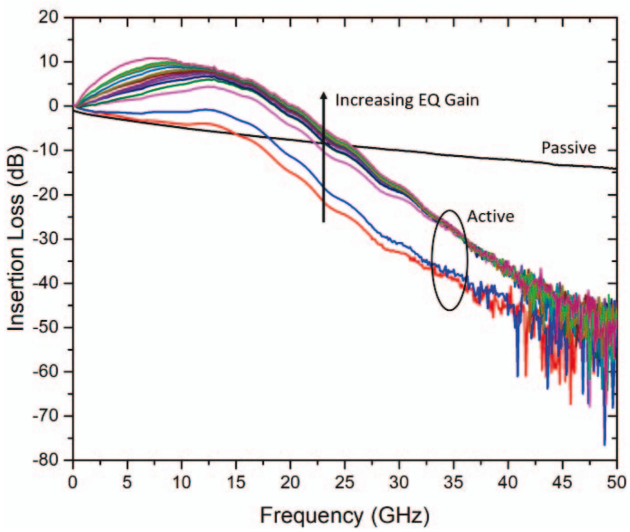

Fig. 6. Insertion loss of active and passive FlexCon channels in the surface mount assembly. Channel length = 44.5 mm.

B. *Active FlexCon*

1) Surface mount assembly

The insertion loss of the surface mount assembly of active FlexCon is shown in Fig. 6. For comparison, the insertion loss of a passive channel of equal length is also provided. Functionality of the redriver was tested by programming the equalization gain to each of the 16 possible settings and measuring insertion loss, demonstrating successful integration of the redriver and passives.

It is important to reiterate that the redriver used here is intended for PCIe 4.0 applications, which has a maximum data rate of 16 Gbps/channel. Thus, the losses in the active channels beyond ~16 GHz are due to limitations of the chip rather than FlexCon. Currently, similar chips are available for PCIe 5.0 applications which support data rates of up to 32 Gbps, the intended FlexCon channel data rate. Upon completion of process development for depackaging and integrating the bare die linear redriver, these components will be implemented. Considering normalized insertion loss at 16 GHz in passive FlexCon channels is 0.148 dB/mm, for operation at 16 Gbps with the redriver implemented here, FlexCon channel reach can be

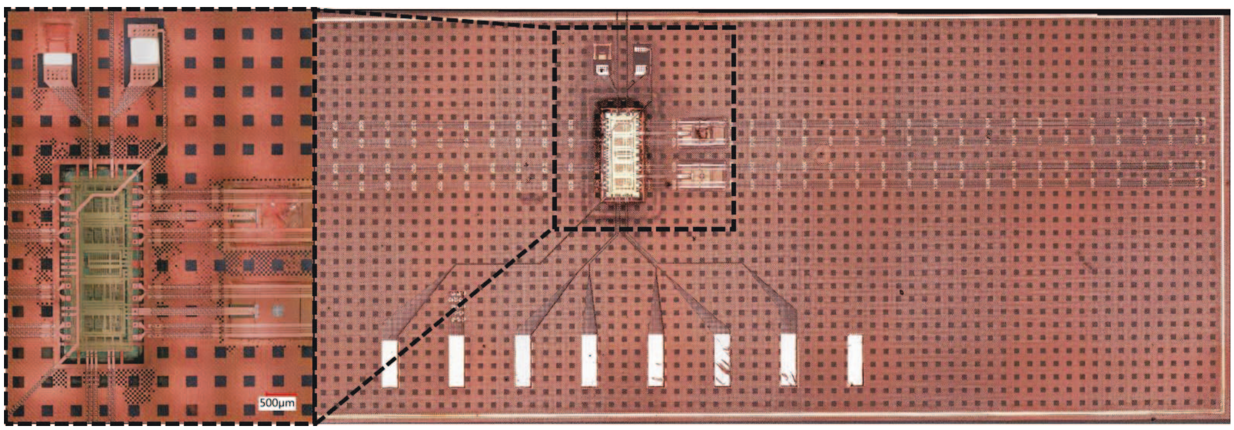

Fig. 7. FlexCon with integrated bare die with epoxy completely removed. Closeup of integrated die and passives on the left to show details.

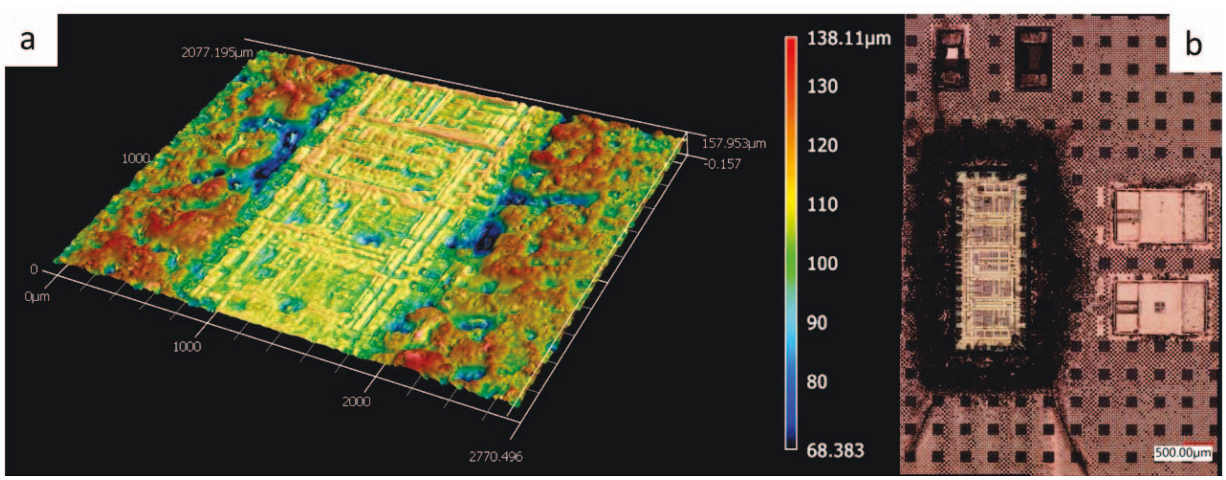

Fig. 8. a) Heat map of topography surrounding depackaged linear redriver with incompletely removed epoxy embedded in PDMS substrate. b) Cracking in FlexCon ground plane due to topography.

extended by ≥60 mm by providing equalization gain of 9.03 dB at 16 GHz, as measured here. At 32 GHz, the normalized loss of passive FlexCon channels is 0.235 dB/mm. Using the TI DS320PR810 as an example of a PCIe 5.0 redriver, which can provide an equalization gain of ~13 dB at 32 GHz [9], the expected improvement to reach for a 32 Gbps implementation is ≥80 mm.

2) Bare die integration

Active FlexCon with integrated depackaged linear redriver and passives is shown in Fig. 7. As stated in Section II, two depackaged die configurations were implemented: un-etched aluminum pads, but remaining epoxy, and etched pads with no epoxy. For the samples with un-etched pads, it was observed that the epoxy remaining on the leadframe resulted in considerable topography in the PDMS following compression molding, as shown in Fig. 8a. The mechanism for this may be due to trapped gases in the epoxy/silica residue. Prior to curing, PDMS sandwiched between the two handling wafers is subjected to vacuum to remove any bubbles. If trapped gas is present in the epoxy, expansion of the gas may push the epoxy toward the die surface, resulting in the topography observed here. The presence of the epoxy residue may also have some effect on the flow of PDMS during molding.

Surface planarity of the PDMS is critical for processing, as topography results in stress concentrations and gradients which can cause cracks in the deposited dielectrics and metals, as well as poor lithography quality. Minimal changes in resistance between the redriver pads and ground during fabrication suggested the die remained functional through the full process. However, the excessive topography caused the formation of cracks, as shown in Fig. 8b, precluding full system functionality.

For the sample in which the aluminum pads on the die were etched during depackaging, resistance measurements could not be performed prior to semi-additive metallization of the die pads. Following pad metallization, it was found that most pads were shorted to ground. It is not known whether the die was damaged prior to this step by, e.g., an ESD event, or if the depackaging process exposed interconnects on the die which were shorted during pad plating. Chemical depackaging techniques in which neither aluminum nor copper are etched have been demonstrated [8], which may be necessary to ensure die functionality prior to integration as well as eliminating topography during PDMS molding.

C. Cyclic mechanical bending

Insertion loss measurements of the passive FlexCon channels with SU-8 dielectric under cumulative mechanical bending are shown in Fig. 9. The percentage change in insertion loss before bending, or "as released", and after 1,000 cycles at 2.5 mm bending radius is shown on the right axis. The percentage change rapidly drops from a peak of 23.1% at low frequency, corresponding to a magnitude difference of 0.232 dB, to <6% at frequencies >10.5 GHz. The maximum magnitude difference was 0.776 dB at 43.8 GHz.

Failure was observed at a bending radius of 1 mm in which the thick SU-8 layer cracked, propagating through the wiring. However, minimal changes in insertion loss were observed at ≥32 GHz for bending radii ≥2.5 mm, suggesting excellent reliability under repeated bending with only minor impact to signal integrity.

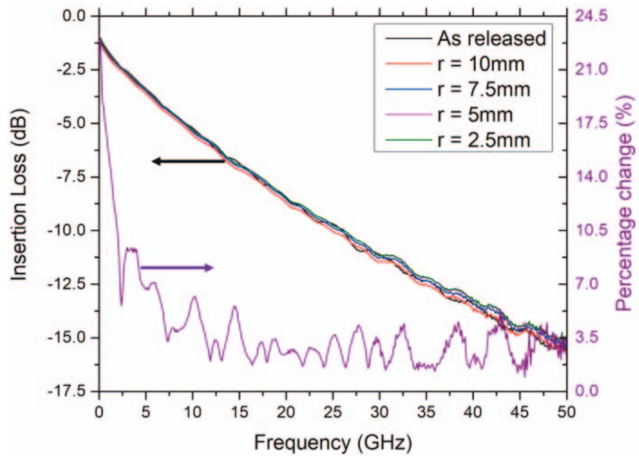

Fig. 9. Insertion loss (left axis) of passive FlexCon channels with SU-8 before and after cumulative bending at radii of 10, 7.5, 5, and 2.5 mm for 1000 cycles each. Percentage change (right axis) between the sample as released and after 1000 cycles at 2.5mm bending radius.

IV. Conclusion

Here we have demonstrated two methods of extending the reach of FlexCon, a high-bandwidth flexible connector for signaling in large area computational systems. First, we have replaced the lossy SU-8 dielectric with low-loss parylene-N, reducing passive channel loss by ~32% at 32 GHz. This enables an additional reach of 12 mm, with an expected reach improvement of 21 mm upon further process optimization. Second, we have implemented an active linear redriver in a surface mount assembly and integrated the depackaged bare die into the FlexCon substrate. The linear redriver provides signal buffering and equalization, enabling an improvement to reach of ≥60 mm at 16 Gbps. Implementation of linear redrivers capable of higher data rates is expected to improve reach by ≥80 mm. Implementing both the parylene-N dielectric and 32 Gbps linear redriver, we expect a total channel reach of ≥120 mm at 32 Gbps, compared to 25 mm for passive channels with SU-8.

Under cyclic mechanical bending, it was found that the change in insertion loss was <6% at frequencies >10.5 GHz after 1000 cycles each of 10, 7.5, 5, and 2.5 mm bending radii. The maximum magnitude change in insertion loss was 0.776 dB at 43.8 GHz. The sample failed at a bending a radius of 1mm.

Acknowledgment

The authors would like to thank the UCLA CHIPS Consortium for their continued support. The authors would also like to acknowledge the facilities and staff of the UCLA Nanolab.

References

[1] S. S. Iyer, S. Jangam and B. Vaisband, "Silicon interconnect fabric: A versatile heterogeneous integration platform for AI systems," in IBM Journal of Research and Development, vol. 63, no. 6, pp. 5:1-5:16, 1 Nov.-Dec. 2019, doi: 10.1147/JRD.2019.2940427.

[2] R. Irwin and S. S. Iyer, "Characterization and design improvement of a high bandwidth, high frequency flexible connector for signal delivery,"

2022 IEEE 72nd Electronic Components and Technology Conference (ECTC), San Diego, CA, USA, 2022, pp. 1759-1763, doi: 10.1109/ECTC51906.2022.00277.

[3] R. Irwin, K. Sahoo, S. Pal and S. S. Iyer, "Flexible connectors and PCB segmentation for signaling and power delivery in wafer-scale systems," 2021 IEEE 71st Electronic Components and Technology Conference (ECTC), San Diego, CA, USA, 2021, pp. 507-513, doi: 10.1109/ECTC32696.2021.00091.

[4] A. Hanna et al., "Extremely flexible (1mm bending radius) biocompatible heterogeneous fan-out wafer-level platform with the lowest reported die-shift (<6 µm) and reliable flexible Cu-based interconnects," 2018 IEEE 68th Electronic Components and Technology Conference (ECTC), San Diego, CA, USA, 2018, pp. 1505-1511, doi: 10.1109/ECTC.2018.00229.

[5] R. G. Pierce, R. Islam, R. M. Henderson and A. Blanchard, "SU-8 2000 millimeter wave material characterization," in IEEE Microwave and Wireless Components Letters, vol. 24, no. 6, pp. 427-429, June 2014, doi: 10.1109/LMWC.2014.2313475.

[6] H. Sharifi, R. R. Lahiji, H. -C. Lin, P. D. Ye, L. P. B. Katehi and S. Mohammadi, "Characterization of parylene-N as flexible substrate and passivation layer for microwave and millimeter-wave integrated circuits," in IEEE Transactions on Advanced Packaging, vol. 32, no. 1, pp. 84-92, Feb. 2009, doi: 10.1109/TADVP.2008.2006760.

[7] G. Ouyang et al., "Comprehensive investigation of in-plane and out-of-plane die shift in flexible fan-out wafer-level packaging using polydimethylsiloxane," in IEEE Transactions on Components, Packaging and Manufacturing Technology, vol. 12, no. 10, pp. 1692-1701, Oct. 2022, doi: 10.1109/TCPMT.2022.3207031.

[8] Lall, P, Deshpande, S, & Nguyen, L. "Fuming acid based decapsulation process for copper-aluminum wirebond system molded with different EMCs." Proceedings of the ASME 2015 International Technical Conference and Exhibition on Packaging and Integration of Electronic and Photonic Microsystems collocated with the ASME 2015 13th International Conference on Nanochannels, Microchannels, and Minichannels. Volume 2: Advanced Electronics and Photonics, Packaging Materials and Processing; Advanced Electronics and Photonics: Packaging, Interconnect and Reliability; Fundamentals of Thermal and Fluid Transport in Nano, Micro, and Mini Scales. San Francisco, California, USA. July 6–9, 2015. V002T01A004. ASME. https://doi.org/10.1115/IPACK2015-48638.

[9] Texas Instruments, “DS320PR810 Eight-channel linear redriver for PCIe 5.0, CXL 1.1” DS320PR810 datasheet, Aug. 2022.